# Self-assembly urethane architecture: Free volume, Connolly surface and diffusion coefficients investigation

Tarek M. Madkour* and Rasha Azzam

***Abstract***- The efficiency of polyurethane foams as thermal insulators depends to a great deal on the permeability of various gas molecules through the urethane polymer with higher temperatures enhancing the diffusion of gas molecules through the polymer. In order to increase the efficiency of these insulators, the design of new urethane polymers with low affinity for diffusing gas molecules such as oxygen, nitrogen and carbon dioxide is necessary. Through maximizing the hydrogen bonding network between the hard blocks and the soft segments in the interface region of the polymeric material, new designs of molecularly organized polyurethanes were achieved in this study and evaluated in terms of their capacity to hinder the permeation of the various gas molecules through the polymer.

***Keywords***- Connolly surface, diffusion, free volume, molecular dynamics, thermal insulators

## I. INTRODUCTION

Subtropical countries enjoy a mild hot weather all around the year with daily temperatures that could reach above 50$^{o}$C in the hot season. Urethane thermal insulators with low densities are perfect materials for this kind of applications. The closed-cell foam structure encompassing the air molecules prevents the thermal conductivity and enhances the efficiency of the used foams as thermal insulators to be used in appliances, construction and automobiles. Polyurethane foams are the insulator of choice in the manufacturing of appliances because of its low thermal conductivity and easy injection into the cavities [1]. Polyurethane foam systems are closed-cell thermosetting plastics characterized by high strength to weight ratio with the primary advantage being outstanding insulating capabilities [1-2]. These are two component systems comprised of isocyanate (hard block) and a resin compound (soft block) that typically contains polyols, catalysts, surfactants, fire retardants and blowing agents [3]. Polyurethane is formed by co-injection of the isocyanate and resin into open or closed molds. The key material property of polyurethane foams in the insulation applications is thermal conductivity.

Manuscript received December 9, 2008: Revised version received December 10, 2009.

The authors are with the Petroleum Chemistry Program of the American University in Nigeria, PMB 2250, Yola, Nigeria.

*Tarek M. Madkour is the corresponding author and may be contacted at tarek.madkour@aaun.edu.ng.

Several research groups have investigated the thermal conduction through gas permeability of rigid polyurethane foams covering both rate of gas diffusion and loss in insulation performance on gas solubility within the foam structure [2], [4-5]. Increased attention is being given to the long-term performance of insulation materials at moderate temperatures [5]. In the case of rigid polyurethane foams, work has mainly focused on the foam performance, as affected by gas diffusion in and out of the cellular structure. In comparison, polyurethane research groups have given less attention to the effects of gas absorption and diffusion at higher temperatures. The very high thermal conductivity of common gases, however, can have considerable detrimental effects on long-term insulation performance if the gases are allowed to build up within the structure of the insulator [6]. Although a considerable literature exists in the area of insulation loss on gas diffusion, much of the information has been created by researchers who often perceive polyurethane (PU) to be a single material and are relatively unaware of the flexibility of the base chemistry [6-7].

The amount of gases including water vapor that can penetrate a PU foam at elevated temperatures was found to be surprisingly high, values over 150% weight increase have been reported in the literature [8]. In work on insulation loss caused by gas penetration, there are two issues that have been reported [9], (i) the overall rate of gas diffusion through the material; and (ii) the effect of the thermal conductivity of the gases on the insulation properties of the material. These can be considered as independent variables but an understanding of both issues is required for the improvement of the product performance. It is apparent from the literature that most examinations of the performance of the insulators were performed at moderate temperatures. The work proposed here seeks to examine the molecular chemistry and architecture of the polyurethane foams and to make use of the variety of the chemical components used to manufacture the polyurethane material in order to generate better polyurethane insulators. This is achieved through using molecular dynamics techniques in order to evaluate the most relevant structural parameters pertaining to the permeability of common gases through PU polymers. Fried and Goyal [10] have similarly applied molecular dynamics techniques for other polymers using the bonded constants in the DREIDING forcefield, which was parameterized using AM1 calculations of dimmer molecules. The bonded constants

were usually validated through the simulation of amorphous cell density and x-ray data (d-spacing) and used to calculate diffusion coefficients and the sorption isotherms for different gases permeating through the polymers. They obtained an excellent agreement for the diffusion and solubility coefficients for $O_2$, $N_2$ and $CH_4$ using the optimised DREIDING forcefield parameters. Trajectory analysis suggested that gas permeation occurs probably through large interchain regions formed by the rigid blocks of PU, which could be well described by the dual-mode model for sorption (S) of gasses in polymers, given by:

$$S \equiv C = K_d a + C'_H \frac{ba}{1+ba} \quad (1)$$

where a is the relative penetrant pressure, p/p* (equal to the thermodynamic activity of an ideal gas). The concentration of penetrant in the polymer (C) has the units of mass of vapor sorbed per mass of polymer. The Henry's law parameter, $K_d$, is identified with penetrant sorption into the densified equilibrium matrix of the polymer, whereas the Langmuir capacity parameter, C′H, characterizes the sorption capacity of the non-equilibrium excess free-volume associated with the glassy state of the polymer. Finally, the Langmuir affinity, b, is an equilibrium constant characterising the affinity of the penetrant for a Langmuir site in the polymer.

## II. METHODOLOGY

For the molecular dynamics study of the various polyurethane systems, a simulation model based on the work of Depner and Schürmann [11] for aromatic polyesters is employed using Materials Studio software package, Molecular Simulation, inc. The polymer segments are subject to the bond-stretching potential, $E_b$:

$$E_b = K_b(l - l_o)^2/2 \quad (2)$$

where $l_o$ is the equilibrium bond length and $K_b$ is the bond stretching constant. The deformation of the bond angle θ between successive pairs of bonds from its equilibrium value o is governed by the potential $E_\theta$:

$$E_\theta = K_\theta (\cos\theta - \cos\theta_o)^2/2 \quad (3)$$

with $K_\theta$ is the bond-bending constant. The torsional potential, $E_\phi$, is modeled as

$$E_\phi = K_\phi (1 + \cos(n\phi - \tau)] \quad (4)$$

where $K_\phi$ is the torsional constant, height of the energy barrier, n is the periodicity and τ the phase angle. Out-of-plane deformations modeled as a special case of the torsion equation with τ = 0 and n = 2 is given by, $E_x$ [11]:

$$E_x = K_x[1 + \cos(2\phi)] \quad (5)$$

The out-of-plane potential acts to keep the connected atom in the plane defined by the other three atoms. $K_x$ is the out-of-plane deformation constant. Non-bonded Lennard-Jones interactions between atoms separated by four bonds or more are given by $E_{nb}$:

$$E_{nb} = 4\varepsilon^* \left[ \left( \frac{r^*}{r_{ij}} \right)^{12} - \left( \frac{r^*}{r_{ij}} \right)^{6} \right] + C \quad \text{for } r_{ij} = 1.5\, r^* \text{ and}$$

$$E_{nb} = 0 \quad \text{for } r_{ij} > 1.5\, r^* \quad (6)$$

The Lennard-Jones parameters between different atoms A and B are assumed to satisfy the Lorentz–Berthelot mixing rules defined by:

$$r_{AB}^* = (r_A^* + r_B^*)^{1/2} \text{ and } \varepsilon_{AB}^* = (\varepsilon_A^* \varepsilon_B^*)^{1/2} \quad (7)$$

where $r^*$ and $\varepsilon^*$ are the Lennard-Jones radius and potential. The electrostatic interactions between atoms carrying partial charges are given by $E_{ij}$:

$$E_{ij} = \frac{q_i q_j}{4\pi\varepsilon r_{ij}} \quad (8)$$

where $q_i$ and $q_j$ are the partial atomic charges on atoms i and j, respectively, $r_{ij}$ is the distance between them and ε is the dielectric constant. The partial charges calculated [10] using the semiemperical molecular orbital method, MNDO, are used. The COMPASS forcefield was used with all hydrogen atoms explicitly considered. A single polymer chain of 500 repeat units was used in order to minimize the effect of chain ends on the results of the simulation. Initial configurations with periodic boundary conditions were generated in the simulation box as to enable the simulations to be carried out on relatively small molecular systems in such a way that the atoms experience forces as if they were in the bulk phase. In order to enhance the sampling efficiency in calculating the diffusion coefficients, ten gaseous molecules of each type were inserted into the cells. This was done to ensure a reliable representation of the trajectories. The equilibrium molecular dynamics simulations were usually performed using microcanonical ensembles. For every structure, the simulations were run several times; usually four runs, for better averaging [12]. The self-diffusion coefficients of the gas molecules were calculated from the Einstein relation [13]:

$$D_o = \frac{1}{6N} \lim_{t\to\infty} \frac{d}{dt} \sum_{i=1}^{N} \left\langle \left[ r_i(t) - r_i(0) \right]^2 \right\rangle \quad (9)$$

where $r_i$ is the position vector of atom i and N is the number of all gas molecules. The angular brackets denote averaging over all choices of time origin and over all particles. The diffusion coefficients of the penetrant molecules were only considered in evaluating the permeability through the different structures.

The systems under study are six molecularly organized PU structures. The molecular organization is normally achieved through the interlocking of the PU chains via the two-dimensional hydrogen bonding network [3]. The basic molecular structure of PU is shown in Fig 1 and is based on either methylene diisocyanates (MDI) or toluene diisocyanates (TDI) as the hard block and polyether polyol (PE), polyester polyol (PST) or hydrocarbon (HC) as the soft block. Every one of the six PU structures is basically a combination of either of the hard blocks and one of the soft blocks. These structures are MDI/PE, TDI/PE, MDI/PST, TDI/PST, MDI/HC, and TDI/HC. This is done in order to highlight the effect of the molecular structural parameters on the diffusion of common gases through PU in order to facilitate the molecular design of excellent PU insulators.

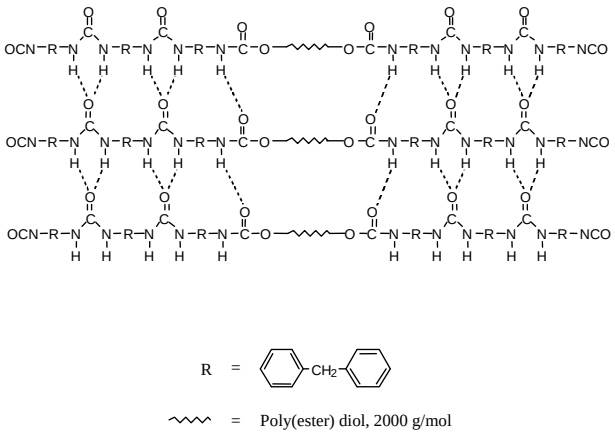


Fig. 1 Molecular representation of the molecularly organized PU samples. The urea groups are locked in register to produce the desired molecular architecture.

## III. RESULTS AND DISCUSSION

In order to investigate the influence of changing the molecular structural parameters on the diffusion coefficients of the various structures, molecular dynamics techniques were used to evaluate the diffusion coefficients of permeating $O_2$, $N_2$ and $CO_2$ molecules through the different polymeric structures. However, specific electrostatic interactions between the various molecules and the polymer might add to the complexity of relating the difference in the diffusion coefficients to the structural parameters of the various systems. Therefore, noble gases are also used in this study since they have little interaction with the polymer and any conclusions about the diffusion of the noble gases into the polymer should be based only on the free-volume effect. The noble gas that will resemble these gases the most should have a Connolly surface of a close value to those of the other gases [14].

### *A. Connolly surface*

A Connolly surface [15] is the van der Waals surface of the model that is accessible to a solvent molecule having a non-zero radius. The surface is generated by rolling a spherical probe of a specified radius over the van der Waals surface of the models. Table 1 lists the Connolly surface of $O_2$, $N_2$ and that of the different noble gases.

Table 1. Connolly surfaces of $O_2$, $N_2$ and various noble gases

| Gas | Connolly surface (Å$^2$) |
|---|---|
| $O_2$ | 42.986 |
| $N_2$ | 40.002 |
| He | 24.630 |
| Ne | 29.802 |
| Ar | 44.415 |
| Kr | 51.276 |
| Xe | 58.630 |

It is apparent from the table that argon has the closest value to that of $O_2$ and $N_2$ for the Connolly surface. Fig 2 is a schematic representation of the Connolly surfaces of Ar and $N_2$.

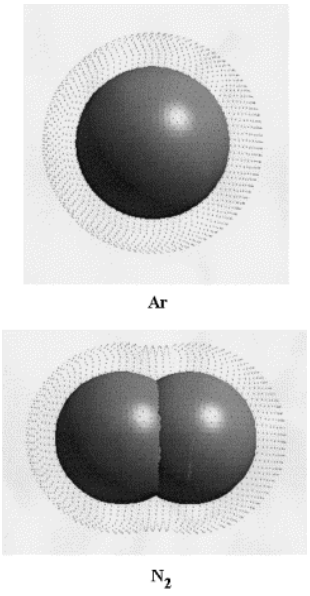


Fig. 2 Schematic presentation of Connolly surfaces of $N_2$ and Ar gas molecules

### *B. The self-diffusion coefficients*

The self-diffusion coefficients for argon, oxygen, nitrogen and carbon dioxide through the various polyurethane systems were determined at the three different temperatures of 25, 35 and 50$^o$C. The calculations were made as outlined previously and are shown in Fig 3-5 for the three different temperatures, respectively. All the calculations were made assuming zero solubility, which is a good assumption for these gasses in the polymeric systems. It could be shown in all the figures that the PU system composed of MDI as the hard block and polyether polyols as the soft block had the highest resistance for the diffusion of the penetrate gases and therefore had the best performance in terms of the thermal insulation. From the figures, it is obvious that the TDI/PE PU system had the second best performance in

terms of thermal insulation where the TDI/HC system showed the highest permeability for the diffusing particles.

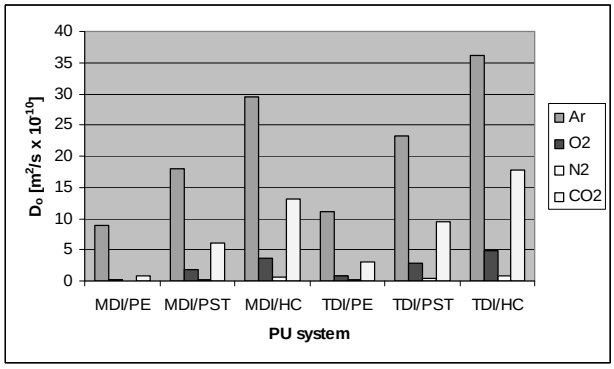


Fig. 3 Self-diffusion coefficients of Ar, $O_2$, $N_2$ and $CO_2$ in PU systems at 25$^o$C.

It is apparent from the figures that the permeability of the PU systems for the various gases is highly influenced by the type of the soft block rather than the type of the hard block. This is probably since the soft block represents 70-80% of the material by weight in addition to the slight structural differences between MDI and TDI as compared to the apparent structural differences between PE, PST and HC.

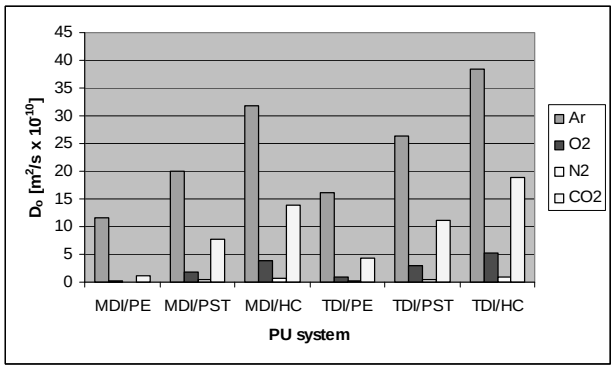


Fig. 4 Self-diffusion coefficients of Ar, $O_2$, $N_2$ and $CO_2$ in PU systems at 35$^o$C.

Interestingly, the various gases under study had produced various results in terms of their diffusion behavior. For example, argon had the highest diffusion coefficient while $N_2$ had the lowest. This is due to their affinity to the polarity of the different PU systems. Unlike the molecules of the other gases, argon is a noble gas and therefore does not possess any electronegative atom.

The motion of the molecules that have electronegative atoms is most likely to be hindered by the on-going repulsion-attraction intermolecular interactions during the diffusion process, which makes it difficult for the gas molecules to jump from one void to another within the polymer network structure in order to complete the diffusion process. Using molecular dynamics techniques, it was possible to show that the chain packing achieved through the 2D-bifuracated hydrogen bonding network is one of the most important molecular structural parameters that influences the polymer to increase its local segment density and subsequently controls its fractional free-volume.

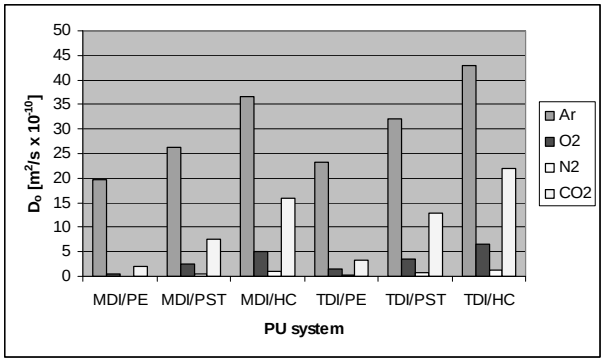


Fig. 5 Self-diffusion coefficients of Ar, $O_2$, $N_2$ and $CO_2$ in PU systems at 50$^o$C.

*C. Free-volume*

In order to study the free-volume size and distribution in bulk simulated molecular models, the hard probe method was used [16-18]. In this method, the periodic box was divided into 100×100×100 cubic subcells. All of the atoms were assumed to be hard spheres with radii equal to 88% of the full van der Waals radii.

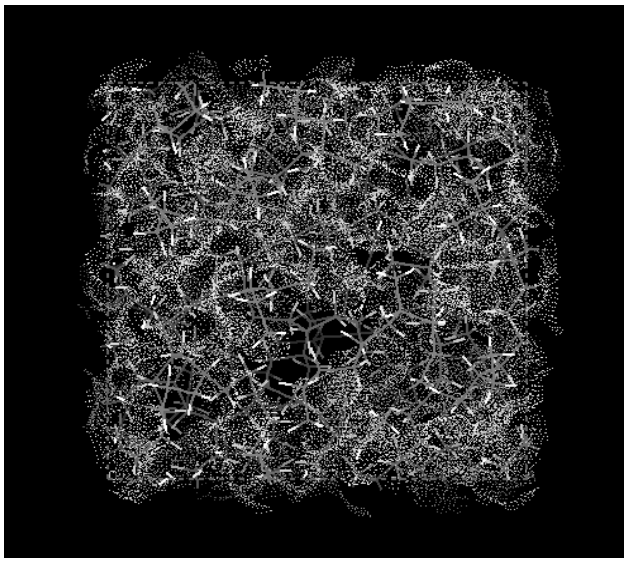

Fig. 6 Schematic representation of an isosurface encompassing the free-volume in a 3D-periodic cell containing a single PU chain.

Each subcell was then scanned to screen out the occupied subcells. The subcell was labelled as "occupied" whenever more than half of the subcell size lay within any hard sphere. After checking occupancy, a probe, which is also assumed to be a hard sphere, was introduced at the centre of an unoccupied subcell. Each

unoccupied subcell was determined to be "inaccessible" if more than half of any occupied subcell size lay within the spherical probe.

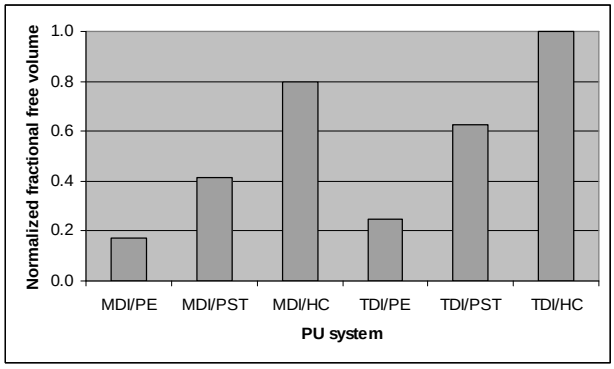


Fig. 7 The normalized fractional free volume values for the various PU systems.

The inaccessible subcells were classified as occupied subcells as well. According to Roe et al. [16] connectivity is formed when two unoccupied subcells having connectivity were assigned to the same void. The total unoccupied volume of the cell divided by the total volume of the cell is thus defined as the fractional free-volume of that cell. Fig 6 shows a schematic representation of an isosurface encompassing the free-volume in a 3D-periodic cell containing a single PU chain. Fig. 7 indicates a comparison between the calculated fractional free-volume of the six different PU structures normalized to the highest value. It is apparent from the figure that varying the molecular structural parameters had a major influence on the free-volume. The ability of the soft block such as PE or PST to form hydrogen bonding presents apparent obstacles against the diffusing molecules, which explains the high diffusion coefficients in case of MDI/HC and TDI/HC PU systems.

Unlike TDI, MDI is a symmetrical molecule capable of forming a molecularly organized bifurcated hydrogen bonding network, Fig 1. This is the maximum hydrogen bonding superstructure that could be found within a PU system, which explains the low diffusion coefficients in case of MDI as opposed to TDI systems.

*D. Energy contour maps*

In order to study the influence of the extra benzyl group in MDI over TDI, energy contour maps for the two MDI/PE and TDI/PE repeat units were calculated for ST and SR pairs of the dihedral angles T, S and R as shown in Figs. 8 and 9. Varying two torsions with respect to each other leads to a potential energy surface that is essential to understand the correlations between the various conformations of neighboring dihedral angles. The energy surface was scanned every $10^{o}$ from $-180^{o}$ to $+180^{o}$. During the generation of the energy contour, the rest of the molecule was minimized by the conjugated gradient method until the energy derivatives were less than 0.001 kcal $mol^{-1}$. Torsion forcing of 1000 kcal $mol^{-1}$ was used to force a torsion systematically to a grid of angles. It is obvious from the figures that the extra phenylene group in the HNA repeat unit didn't influence the location of the local minima in both cases to a great deal. Therefore, it must be expected that the population of the trans and gauche states should be similar for both polymers.

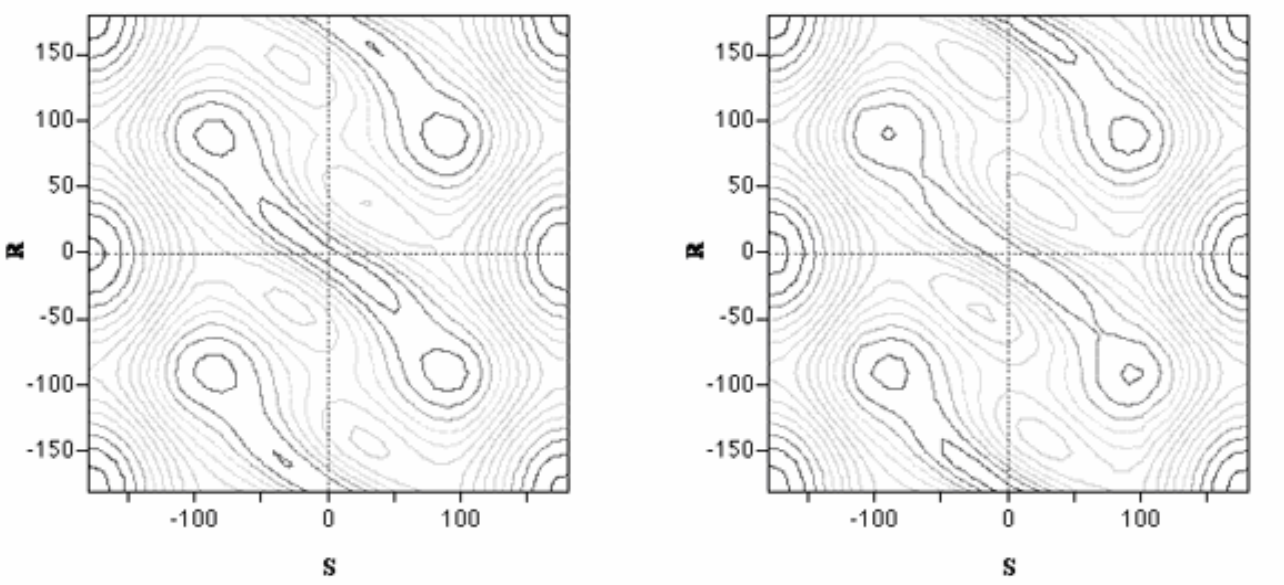


Fig. 8 Energy contour maps displaying the potential energy as a function of rotation around torsional angles R and S.

The rotations around the S bond change the shape of the chain which means the torsional behavior of the S bond is the most important from the viewpoints of polymer flexibility and processability. The energy barrier

height for rotation around the S bond was found to be more than 11.9 kcal $mol^{-1}$ implying that rotation is more restricted in this case than the one around the R bond which was estimated to be of 5.59 kcal $mol^{-1}$. The methylene linkage thus provides little opportunity for the chain to exhibit a configurational flexibility. The conformational energy calculations indicate that the phenylene group attached through the T bond is prevented from rotating into the same plane of urea/urethane groups by steric interaction between neighboring groups caused by the formation of the hydrogen bonds.

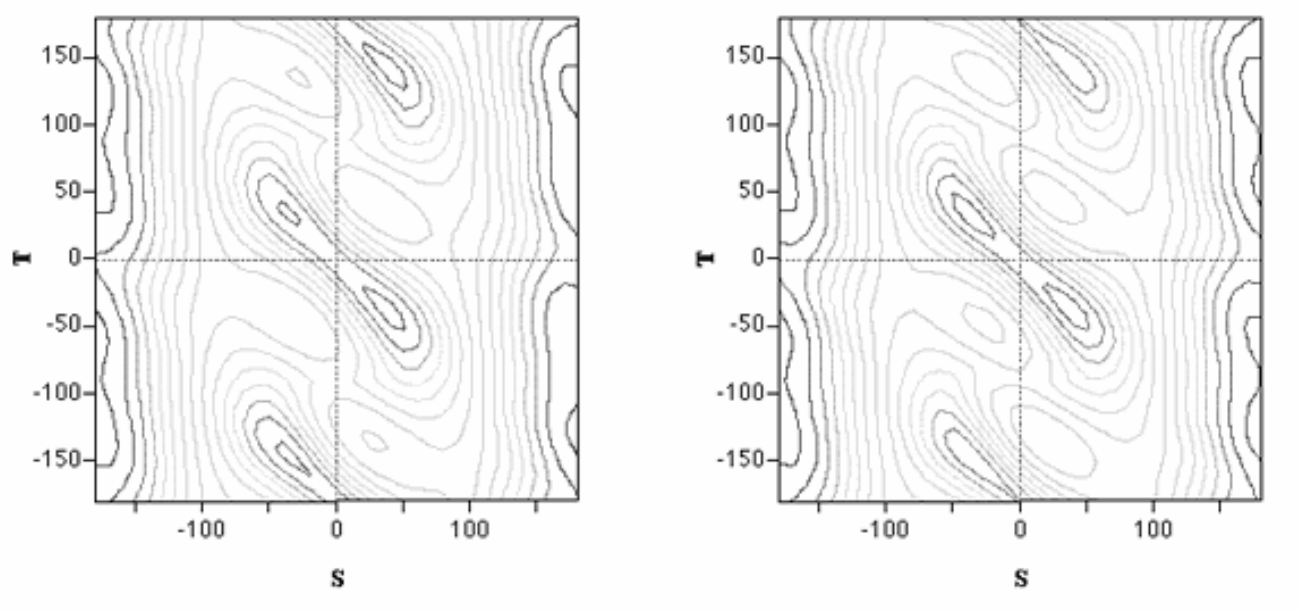


Fig. 9 Energy contour maps displaying the potential energy as a function of rotation around torsional angles S and T.

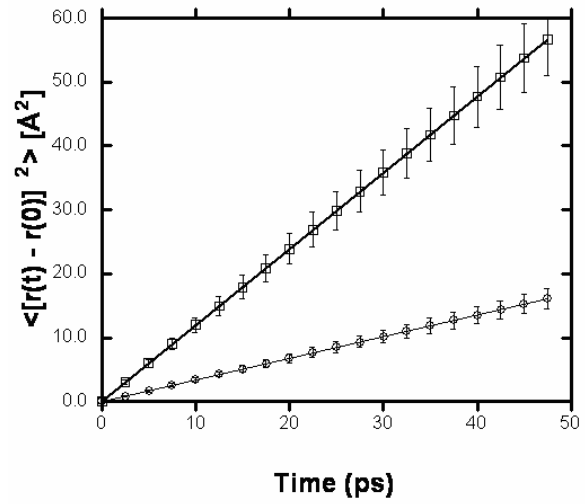


Fig. 10 The evolution of the mean square displacement for MDI/PE at 25°C

The side step associated with the methylene group provides an additional measure of conformational freedom through crankshaft type motions associated with rotations around R and T bonds causing the second phenyl group to move laterally with respect to the first in case of PU polymers synthesized using MDI.

*E. Mean square displacements*

Results of the molecular dynamics are all shown in Figs. 10 through 18.

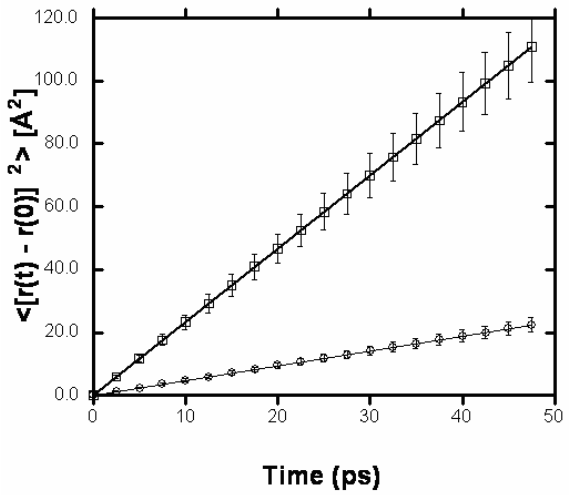


Fig. 11 The evolution of the mean square displacement for MDI/PE at 35°C

The different figures clearly show the evolution of the mean square displacement as a function of time for the diffusing gas molecules and the polymer molecules for the three MDI PU systems, which showed the lowest self-diffusion coefficients at the different temperatures. It should be obvious from the figures that increasing the

temperature had a proportional effect on the mean square displacement due to the increase in the kinetic energy available to the systems.

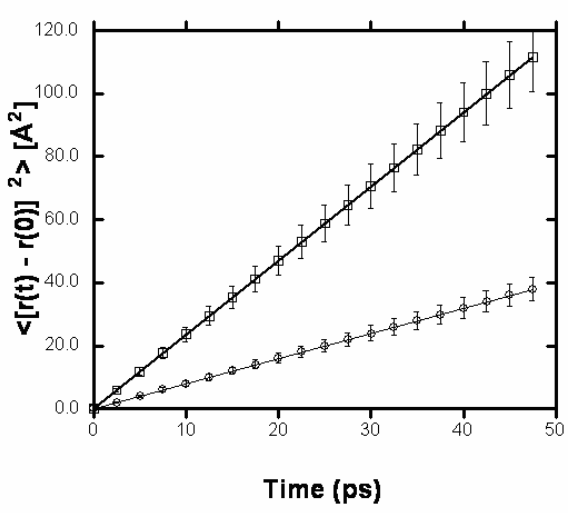


Fig. 12 The evolution of the mean square displacement for MDI/PE at 50°C

Both polar polymers (MDI/PE and MDI/PST) did have very low values of the mean square displacement as compared to the nonpolar hydrocarbon MDI/HC.

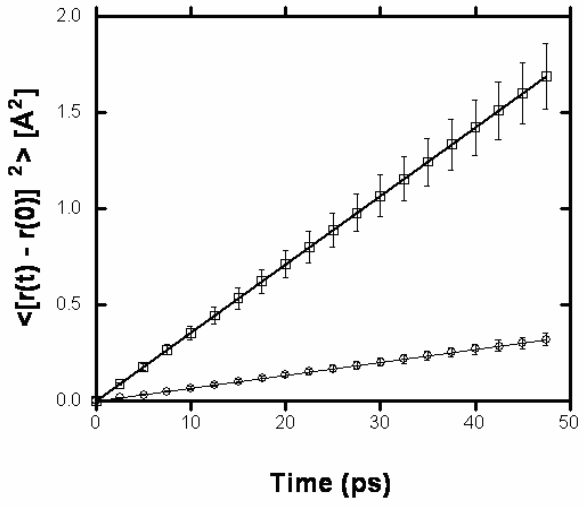


Fig. 13 The evolution of the mean square displacement for MDI/PST at 25°C

It could be thus deduced that the conformational properties of the polymeric chains in relation to its flexibility have an impact on the self-diffusion coefficients of the penetrating gas molecules through a certain polymer. This is due to the inflexibility of the polymeric chain, which hinders its movement as well as the movement of the gas molecules. It could also be observed that at the highest temperature, the MDI/PST molecules have similar values for the mean square displacement to those of the gas molecules. This is since the polymer in this case has the dense bifurcated hydrogen bonding network. Nevertheless, in case of the MDI/HC polymer, it is shown that at lower temperatures, both the polymer and the gas molecules have similar values for the mean square displacement.

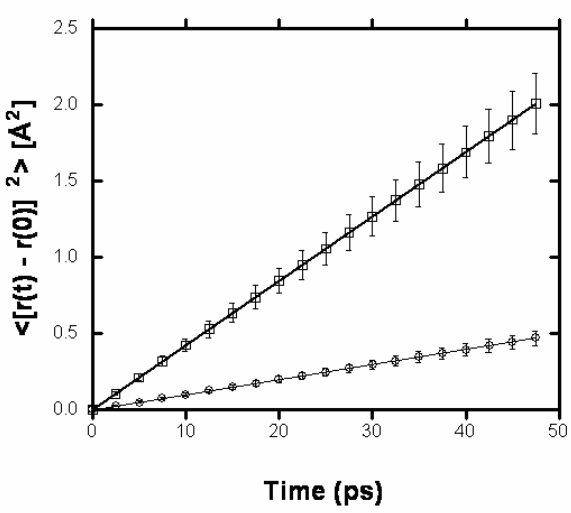


Fig. 14 The evolution of the mean square displacement for MDI/PST at 35°C

The similar values for the mean square displacement indicate similar self-diffusion coefficients.

*F. Numerical Simulations of the Urea Formation*

Numerical simulation techniques based on Monte Carlo methods [19] are used to simulate the reactions between the various components of the reaction mixture and to predict the influence of using higher loadings of a blowing catalyst on the hard segment content and the amount of the urea content within the formed hard segments.

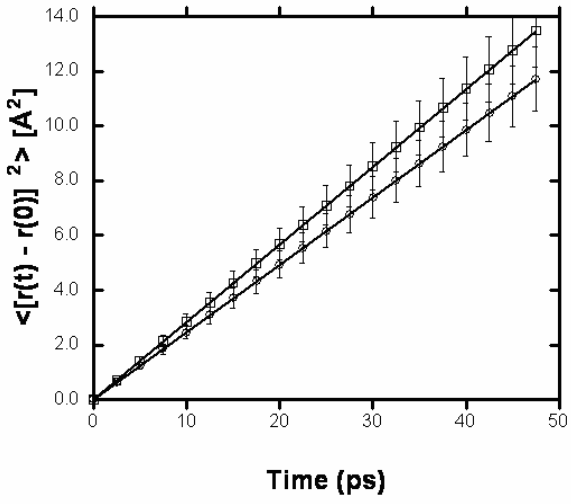


Fig. 15 The evolution of the mean square displacement for MDI/PST at 50°C

The numerical calculations involve the simulation of a virtual reaction pot containing all the various ingredients of the experimental one-shot system. 100,000 molecules

are thus simulated in accordance with the molar ratio of the various components of the one-shot formulations. Molecules are chosen at random for reaction using a random number generator and applying the Monte Carlo methods. If the reaction is unsuccessful, the molecules are returned to the pot for further attempts.

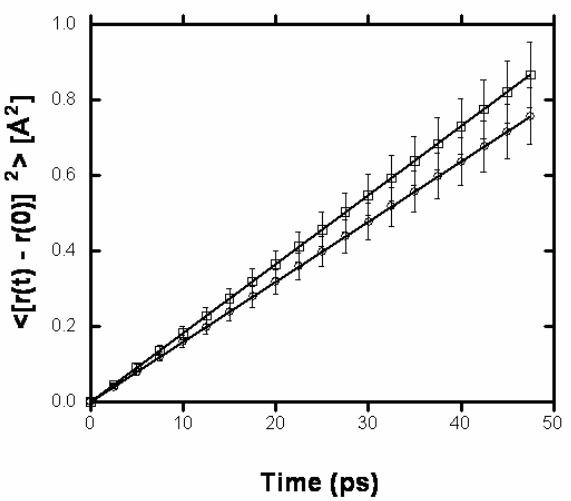


Fig. 16 The evolution of the mean square displacement for MDI/HC at 25°C

All hydroxyl groups residing either on the polyol molecules or on the chain extenders have been assumed to have equivalent reactivities. The chemical reactions between the hydroxyl and isocyanate groups result into urethane linkages. Water was also allowed to react in this case with the isocyanate groups to produce amine and carbon dioxide.

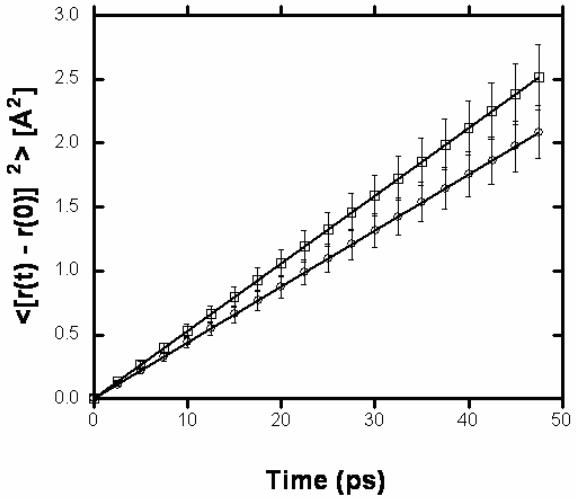


Fig. 17 The evolution of the mean square displacement for MDI/HC at 35°C

This is since the produced amino compounds are then re-entered into the virtual pot and are allowed to participate in the overall reaction scheme through their rapid reaction with other isocyanate groups to produce urea linkages between the virtual reacting molecules. The relative reaction rates of the various reactions were taken as follows:

NCO/amine : NCO /hydroxyl : NCO /water = 10 : 2 :1

By continuously re-adjusting the relative NCO/water reaction rate, the effect of the blowing catalyst could thus be simulated. Information on the distribution of the hard segments and the urea linkages were collected throughout the simulation runs and stored for later analysis.

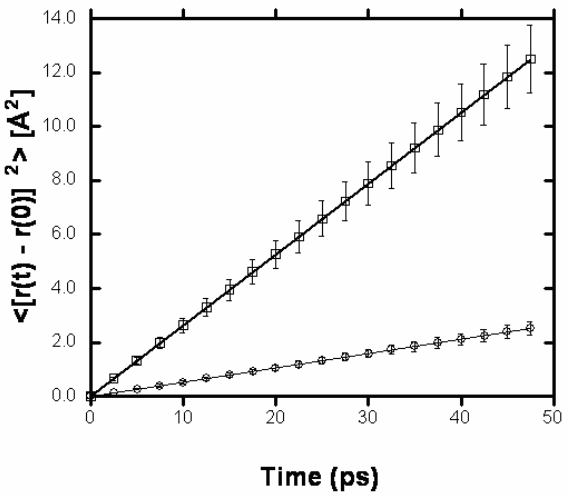


Fig. 18 The evolution of the mean square displacement for MDI/HC at 50°C

Figs. 19 and 20 indicate that, theoretically, the higher the loading of the Niax A99 catalyst the higher the amount of the hard segment content within the final foam.

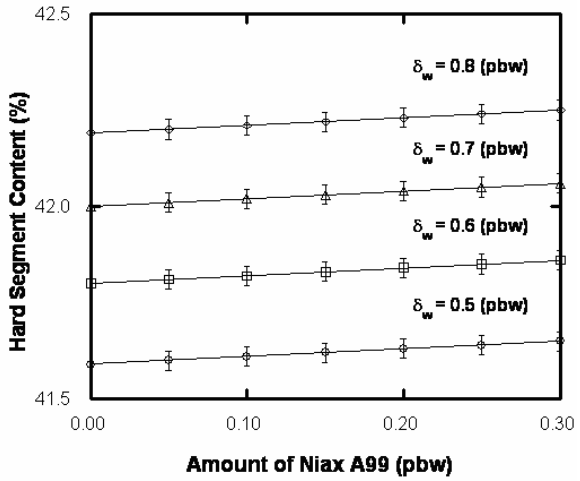


Fig. 19 Numerical simulation of the hard segment content of PU polymers as a function of the amount of blowing catalyst

Fig. 20, however, illustrates the influence of increasing the water and blowing catalyst contents on the amount of urea groups in the hard domains. In the theoretical calculations, the effect of the exotherm on the

evaporation of the water molecules is not taken into account. The figure predicts the greater influence of the blowing catalyst at higher water contents on the formation of the urea groups in complete agreement with the experimental observation, as more water molecules will have a greater chance to participate in the urea formation reactions.

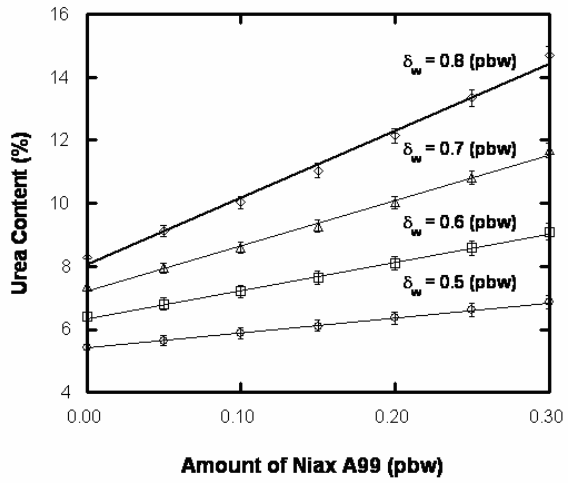


Fig. 20 Numerical simulation of the urea group content in the hard block of PU polymers as a function of the amount of blowing catalyst

This is interesting since Fig. 20 represents the ideal behavior of the blowing reactions in terms of the produced urea content. A simple comparison between the simulated results and actual data [19] illustrates the deviation of the various studied systems from ideality due to (i) the influence of the exotherm on the evaporation of water, (ii) the increasing incompatibility between the growing polymer chains and the existing water molecules, and (iii) the hydrogen bonding formation between the newly created urea/urethane groups and the existing water molecules.

*G. Polymer self-assembly*

Polymers satisfy the size requirement for many potential nanotechnologies and are an example of chemically directed self-assembly. Owing to their mutual phase separation, dissimilar hard and soft blocks of a PU polymer may mimic olefin diblock or triblock copolymers, which tend to segregate into different domains. The spatial extent of the domains is limited by the constraint imposed by the chemical connectivity of the blocks, hence is quite interesting to study the ways olefin diblock and triblock copoylymers self-assemble. Area minimization at the interface of the two blocks takes place to lower the interfacial energy. From an entropic standpoint, the molecules prefer random coil shapes but the blocks are stretched away from the interface to avoid unfavorable contacts. As a result, of these competing effects, self-organized periodic microstructures emerge on the nanoscopic length scale. As shown in Fig. 6(a), for nearly symmetric diblocks, a lamellar phase occurs. For moderate compositional asymmetries, a complex bicontinuous state, known as the double gyroid phase, has been observed in which the minority blocks form domains consisting of two interweaving threefold-

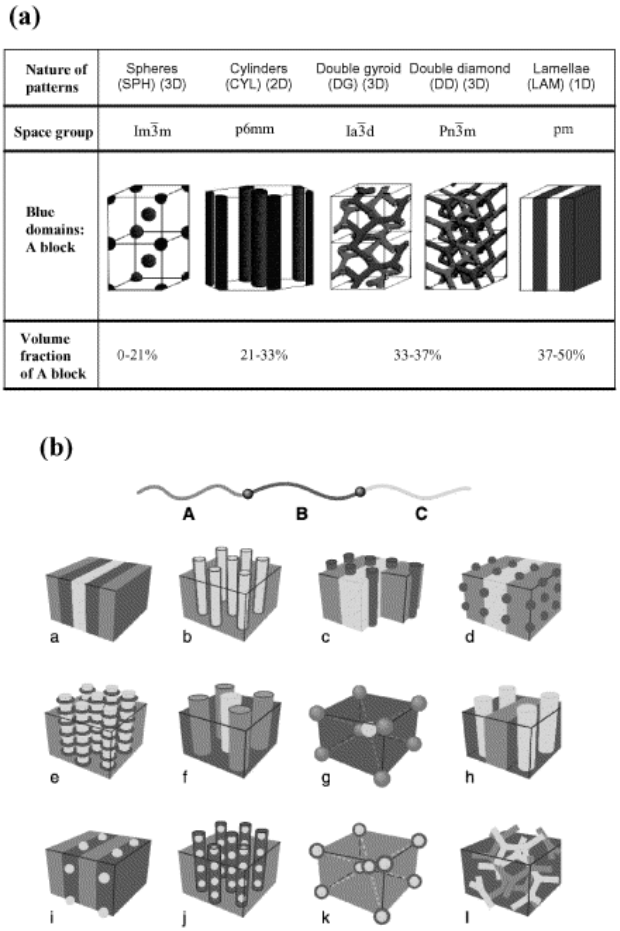


Fig. 6 (a) Schematic phase diagram showing the various `classical' olefin copolymer morphologies adopted by noncrystalline linear diblock copolymer. (b) Schematic of morphologies for linear ABC triblock copolymer.

coordinated networks. At yet higher compositional asymmetry, the minority component forms hexagonally packed cylinders and then spheres arranged on a body-centered cubic lattice and a homogeneous phase results. The equilibrium morphologies of ABC triblock terpolymers are more diverse than those of AB diblock copolymers (Fig. 6(b)). In ABC triblock terpolymers, there exist two composition variables and three interaction parameters, which make their phase behaviors much more complicated than AB diblocks having only one composition variable and one interaction parameter.

## IV. CONCLUSION

Various polyurethane systems based on different combinations of hard and soft blocks were subjected to a

molecular modeling study for the simulation of the self-diffusion coefficients of various gases representing the air components to determine the best PU insulator. The design of the PU systems ensured molecularly organized urethane interfaces through the maximizing of a bifurcated hydrogen bonding superstructure. Using molecular dynamics techniques, it was possible to show that the chain packing is one of the most important molecular structural parameters that influences the polymer to increase its local segment density and subsequently controls its fractional free-volume. It was shown that MDI/PE PU system had the best insulation performance due to the presence of hydrogen bonding network which hindered the motion of the diffusing molecules and prevented them from jumping from one void to another within the polymeric systems. Replacement of the symmetrical MDI hard block with the less symmetrical TDI has resulted into the disturbance of the hydrogen bonding network and an apparent increase in the self-diffusion coefficients of the various air components. Replacement of the polyether polyol soft block with hydrocarbon soft block has resulted also into an apparent increase in the self-diffusion coefficients, most probably due to the inability of the hydrocarbon material to form hydrogen bonds.

## REFERENCES

[1] G. Biesmans, M. Karremans, D. Randall and S. Singh, J. Cellular Plastics 34 (1998) p. 349.
[2] G. Biesmans, Cellular Polymers 13 (1994), p. 292.
[3] T. Madkour and R. Azzam, J. Polym. Sci. Part A: Polym. Chem. 40 (2002), p. 2526.
[4] A. Cunningham, D. Sparrow, I. Rosbotham and G. Du Cause de Nazelle, 32nd Annual Polyurethanes Technical Conf. Tokyo, Japan, pp. 56, 1989.
[5] W. Tobiasson, A. Greatorex and D. van Pelt, Intl. Symp. Polyurethanes Technology, pp. 383, 1991.
[6] W. Tobiasson, A. Greatorex and D. van Pelt, J. Thermal Insulation, 11 (1987), p. 108.
[7] C. Ming, X. Zeng and L. Ye, ASHRAE Transactions, 103 (1997), p. 309.
[8] F. Dechow and K. Epstein, Thermal Transmission Measurements of Insulation. ASTM STP 660. Ed. R. P. Tye. American Society for Testing and Materials, pp. 234, 1978.
[9] M. Levy, J. Cellular Plastics, 2 (1966), p. 37.
[10] J. Fried and D. Goyal, J. Polym. Sci. Part B: Polym. Phys. 36 (1998), p. 519.
[11] M. Depner and B. Schürmann, Polymer 33 (1992), p. 398.
[12] F. Cecconi, C. Guardiani and R. Livi. Proceedings of the 2006 WSEAS International Conference on Mathematical Biology and Ecology, Miami, Florida, USA, January 18-20, (2006), pp. 25-30.
[13] M. P. Allen and D. J. Tildesley, Computer simulation of liquids, Clarendon Press, Oxford, 1987.
[14] T. M. Madkour, Polymer 41, (2000), p. 7489.
[15] M.L. Connolly. J Appl Crystallogr 16 (1983), p. 548.
[16] D. Rigby and R.J. Roe. Macromolecules 23 (1990), p. 5312.
[17] H. Vladimr, L. Karel. WSEAS Transactions on Electronics 4(9) (2007), pp. 181-185.
[18] J. Janela, A. Sequeira and F. Carapau. Proceedings of the 2006 IASME/WSEAS International Conference on Continuum Mechanics, Chalkida, Greece, May 11-13, (2006), pp. 85-90.
[19] Madkour, T. M., Azzam, R. A., Journal of Polymer Science Part A: Polymer Chemistry, 40(14), 2526-2536, 2002.